



1 **Ultrasonic Nebulization for the Elemental Analysis of**
2 **Microgram-Level Samples with Offline Aerosol Mass**
3 **Spectrometry**

4
5 Rachel E. O'Brien^{1*}, Kelsey J. Ridley², Manjula R. Canagaratna³, John T. Jayne³, Philip L.
6 Croteau³, Douglas R. Worsnop³, Sri Hapsari Budisulistiorini^{4†}, Jason D. Surratt⁴, Christopher L.
7 Follett⁵, Daniel J. Repeta⁵, Jesse H. Kroll²

8
9 [1] Department of Chemistry, College of William and Mary, Williamsburg, Virginia, 23185, USA
10 [2] Department of Civil and Environmental Engineering, Massachusetts Institute of Technology, Cambridge,
11 Massachusetts 02139, USA
12 [3] Center for Aerosol and Cloud Chemistry, Aerodyne Research Inc., Billerica, Massachusetts 01821, USA
13 [4] Department of Environmental Sciences and Engineering, Gillings School of Global Public Health, University of
14 North Carolina at Chapel Hill, Chapel Hill, North Carolina 27599, USA
15 [5] Department of Marine Chemistry and Geochemistry, Woods Hole Oceanographic Institution, Woods Hole,
16 Massachusetts 02540, USA

17
18 † Now at: Earth Observatory of Singapore, Nanyang Technological University, Singapore 638789, Singapore
19

20 Corresponding author: Rachel O'Brien, reobrien@wm.edu

21

22 **Abstract.** The elemental composition of organic material in environmental samples – including atmospheric organic
23 aerosol, dissolved organic matter, and other complex mixtures – provides insights into their sources and environmental
24 processing. However, standard analytical techniques for measuring elemental ratios typically require large sample
25 sizes (milligrams of material or more). Here we characterize a method for measuring elemental ratios in environmental
26 samples, requiring only micrograms of material, using a Small Volume Nebulizer (SVN). The technique uses
27 ultrasonic nebulization of samples to generate aerosol particles (100-300 nm diameter), which are then analyzed using
28 an aerosol mass spectrometer (AMS). We demonstrate that the technique generates aerosol from complex organic
29 mixtures with minimal changes to the elemental composition of the organic and that quantification is possible using
30 internal standards (e.g., NH₄¹⁵NO₃). Sample volumes of 2-4 μL with total solution concentrations of at least 0.2 g/L
31 form sufficient particle mass for elemental ratio measurement by the AMS, despite only a small fraction (~0.1%) of
32 the sample forming fine particles while the remainder end up as larger droplets. The method was applied to aerosol
33 filter extracts from the field and laboratory, as well as to dissolved organic matter (DOM) from the North Pacific
34 Ocean. In the case of aerosol particles, the mass spectra and elemental ratios from the SVN-AMS agree with those
35 from online AMS sampling; similarly, for DOM, the elemental ratios determined from the SVN-AMS agree with
36 those determined using combustion analysis. The SVN-AMS provides a platform for the rapid quantitative analysis



37 of the elemental composition of complex organic mixtures and non-refractory inorganic salts from microgram samples
38 with applications that include analysis of aerosol extracts, and terrestrial and atmospheric dissolved organic matter.

39 **1 Introduction**

40 A large number of environmental systems, including the atmosphere, natural waters, and terrestrial systems,
41 contain complex organic mixtures composed of hundreds to thousands of molecular species. Our ability to understand
42 and model such complex chemical systems is often greatly improved when we characterize them in terms of simple
43 chemical frameworks. On the simplest level, the analysis of average elemental ratios can provide important
44 information on potential sources of organic matter samples, as well as the chemical and/or biological transformation
45 processes that modify their composition. For example, the elemental ratios of atmospheric organic aerosol – e.g.,
46 oxygen/carbon ratio (O:C), hydrogen/carbon ratio (H:C), and nitrogen/carbon ratio (N:C) – provide information on
47 aerosol sources and aging (Aiken et al., 2008; Canagaratna et al., 2015; Chen et al., 2015; Daumit et al., 2013; Heald
48 et al., 2010; Jimenez et al., 2009; Kroll et al., 2011). Similarly, in water and soil samples, the elemental ratios of
49 carbon, nitrogen, and phosphorous reveal insights into sources and processing of dissolved and particulate organic
50 matter (Becker et al., 2014; Hansman et al., 2015; Koch et al., 2005; Lu et al., 2015).

51 The most widespread technique for elemental analysis is high-temperature combustion followed by elemental
52 (CHNS) analysis, which is highly accurate but can require milligrams of material (Skoog et al., 1998). For many trace
53 environmental samples, like atmospheric aerosol, this can require extremely long collection times which lead to low
54 time resolution, limiting the amount of information provided for systems that exhibit high temporal variability. An
55 alternative approach for measuring the elemental ratios of aerosol is online (real-time) techniques. The most widely-
56 used instrument for such measurements is the Aerodyne High-Resolution Time-of-Flight Aerosol Mass Spectrometer
57 (HR-ToF-AMS) (Decarlo et al., 2006), which can measure elemental ratios of ambient aerosol using just nanograms
58 of material. Over the last decade, in-situ analysis of aerosol particles with the AMS has enabled rapid, sensitive
59 characterization of aerosol concentrations, sources, and atmospheric aging, improving our ability to model
60 atmospheric aerosol and consequently its climate and health effects (Kroll et al. 2015; Ng et al. 2011; Jimenez et al.
61 2009; Canagaratna et al. 2007).

62 Recently, a number of researchers have used the AMS in an “offline mode,” in which atmospheric samples
63 are collected on filters, extracted, and then atomized into the AMS. Examples include the analysis of sources and
64 aging of atmospheric organic material from aerosol filter extracts (Bozzetti et al., 2017; Huang et al., 2014; Sun et al.,
65 2011; Xu et al., 2015; Ye et al., 2017), cloud/fog water samples (Kaul et al., 2014; Lee et al., 2012), and organic
66 material in glaciers (Xu et al., 2013). Offline AMS has proven especially useful for the analysis of aerosol particles
67 larger than 1 μm (Bozzetti et al., 2016; Daellenbach et al., 2016; Ge et al., 2017). Offline AMS has also proven useful
68 in investigating fractionation and solubility of atmospheric organic material in water and organic solvents
69 (Daellenbach et al., 2016; Mihara and Mochida, 2011). These studies used both custom-made and commercial
70 atomizers with solvent volumes of at least 5-15 mL. To generate aerosol particles in the size range needed for the
71 AMS, this corresponds to necessary sample masses on the order of 50 μg . While this represents a substantial
72 improvement over the sample mass requirements of conventional CHNS analysis, it is still sufficiently large to limit



73 the applicability of the approach since it can require relatively large organic samples collected with high-volume
74 samplers, often over 24 hours or more.

75 In this work, we characterize a new technique for the elemental analysis of very small sample masses, using
76 ultrasonic nebulization. Aerosol generation with a small volume nebulizer (SVN) expands the range of environmental
77 samples that can be measured, where either sample size is limited or solvent contamination is a concern. The SVN
78 generates aerosol suitable for analysis with aerosol instrumentation, including not only the AMS but also Scanning
79 Mobility Particle Sizers (SMPS); single particle mass spectrometers (e.g. Particle Analysis by Laser Mass
80 Spectrometry (PALMS) (Murphy et al., 1998)); soft ionization sources (e.g. Extractive Electrospray Ionization (EESI)
81 (Gallimore and Kalberer, 2013)); and thermal desorption chemical ionization mass spectrometers (e.g. Filter Inlet for
82 Gases and AEROSols, (FIGERO-CIMS) (Lopez-Hilfiker et al., 2014)). Here, we present results characterizing the
83 SVN using an HR-ToF-AMS and an SMPS and demonstrate production and elemental analysis of aerosol using 2-4
84 μL of liquid samples, with masses of organic material as low as $\sim 0.4 \mu\text{g}$. Quantification of total organic concentrations
85 is demonstrated using internal standards. We examine the effects of aerosol collection, extraction, and nebulization
86 on the mass spectra and elemental ratios observed for offline and online AMS. The aim of this work is to demonstrate
87 that offline analysis of organic mixtures with the SVN-AMS can provide quantitative characteristic elemental ratios
88 for trace environmental and biological samples using just micrograms of sample.

89 **2 Experimental**

90 **2.1 Small Volume Nebulizer**

91 The SVN, shown in Figure 1, creates an aerosol by ultrasonically nebulizing a small droplet placed on a thin
92 film stretched across a water reservoir. The aerosol is then carried by a gentle flow of either house air or argon (Airgas,
93 99.999% purity) into the AMS. The three main components of the SVN, described in detail below, are (1) a bottom
94 cylinder with an ultrasonic transducer and water bath, (2) a thin film that is press-fit onto the top of the water bath by
95 an upper cylinder with a slightly larger ID, and (3) a vertical glass tube that connects to the AMS. The connections
96 between all components are airtight, but the apparatus is easily disassembled to inject samples onto the film, as well
97 as to clean the thin film and change the water bath.

98 In the bottom section of the SVN, the 2.4 MHz ultrasonic transducer (Sonaer, Inc., Model 241VM) is located
99 just under the liquid reservoir, with a thin film stretched across the top of the reservoir to provide a clean nebulization
100 surface for the sample. We use a 0.001" thick Kapton film or Teflon film, as these two were found to have the lowest
101 background signal and the best performance in terms of the amount of aerosol generated compared to other materials
102 tested. Press-fit onto the bottom piece is another PVC cylinder that has two side ports with carrier gas inlets, and a
103 larger hole in the top into which a 15 cm glass tube is seated. The distance from the thin film to the bottom of the glass
104 tube is ~ 1.5 cm. During experiments, the nebulized aerosol is carried up through the vertical glass tube, into the
105 stainless steel tubing that leads to the AMS. Additional components such as NafionTM (Perma Pure LLC) driers can
106 be placed inline if desired, but such modifications were not investigated in the present work.



107 Samples can be introduced into the SVN using two different approaches: discrete injections of individual
108 samples (for individual “one-shot” measurements) or continuous addition of a sample flow (for continual analysis,
109 enabling signal averaging). For most studies, MilliQ water was used as the solvent; in some cases we used HPLC-
110 grade methanol, though the organic background signal is higher in that case, likely due to a combination of increased
111 organic background in organic solvents and incomplete evaporation of methanol prior to measurement. For most of
112 the work described here, we used discrete injections of 2-5 μL of aqueous solutions manually deposited directly onto
113 the center of the Kapton film. For continuous injections, solutions made with MilliQ or organic solvents were
114 introduced via a syringe pump (Harvard Apparatus Model 22), which sends liquid flow (20-40 $\mu\text{L}/\text{min}$) through a
115 borosilicate capillary entering the SVN via a small downward-facing hole in the upper PVC piece (Figure 1). In the
116 future, such a port could also be used to provide automated discrete sample introduction using an autosampler.

117 For aqueous samples containing salts and small organic molecules, only 1-2% of the original sample mass
118 was observed to remain on the thin film after a discrete injection (Figure S2). To ensure a clean surface between
119 different samples, the surface was cleaned by nebulizing 2-8 μL of MilliQ water off the surface 5-10 times over
120 approximately one minute. The cleanliness of the surface was then verified by running a salt solution (at least 0.5
121 g/L) between each sample. The salt solution is necessary to ensure that any contaminants can be seen, since pure water
122 risks generating aerosol particles that are too small to be measured in the AMS. For samples in which carryover was
123 observed (for example, the dissolved organic matter solutions discussed in section 3.1), additional cleaning of the film
124 was undertaken with sonication in a deionized water bath followed by rinsing with HPLC-grade methanol for > 30
125 seconds. Careful maintenance of the surface ensures uncontaminated mass spectra and accurate quantification of the
126 solution components.

127 2.2 AMS Data Collection and Analysis

128 While a number of different aerosols instruments could be used with the SVN, here we focus primarily on
129 elemental analysis by the HR-ToF-AMS. The AMS has previously been described in detail (Canagaratna et al., 2007;
130 Decarlo et al., 2006) and provides quantitative measurements of non-refractory material (organics, ammonium sulfate,
131 ammonium nitrate, etc.) for aerosol particles between approximately 40 and 1,000 nm. The mass spectrometer used
132 in the AMS is a high resolution time-of-flight mass spectrometer (HToF-MS, ToFwerk AG), run under “V mode” for
133 a mass resolution of 2,000-3,000 $m/\Delta m$. This mass-resolving power enables peak fitting and identification of all
134 organic fragment ions observed here ($< 130 m/z$), which enables the calculation of quantitative elemental ratios for
135 the organic mixture, after correcting for fragmentation bias during electron ionization (Aiken et al., 2007, 2008;
136 Canagaratna et al., 2015). For AMS data collected using indoor or outdoor air, the intensities of CO^+ and H_2O^+ are
137 complicated by gas-phase interferences (N_2^+ and gas-phase H_2O^+). For samples compared to chamber or ambient
138 online-AMS data sets, house air was the carrier gas and standard empirical estimates were used (Canagaratna et al.,
139 2015). With the SVN, inert carrier gases such as argon can also be used, allowing for the direct measurement of the
140 CO^+ ion intensity (as demonstrated below for dissolved organic matter).

141 For discrete sampling, “fast MS” mode (Kimmel et al., 2010) was used because the pulse length of a single
142 injection is ~30-60 seconds long. Fast MS mode generates mass spectra every 0.5-2 seconds and the instrument cycles



143 between the “closed” state, in which the aerosol beam is blocked, and the “open” state, in which the aerosol beam can
144 reach the vaporization/ionization region for detection. For the work shown here, mass spectra were collected every
145 0.5 seconds for ~15-18 seconds in the “open” state, followed by 3 seconds in the closed state. The closed spectrum
146 provides information on the instrument background, including contributions from gas phase species, and is subtracted
147 from the open spectrum in data processing. For continuous injections, the standard AMS operating mode (“GenAlt
148 mode”) was used. This provides an average mass spectrum (by subtracting the closed signal from the open signal), as
149 well as particle time-of-flight (PToF) data (providing aerosol size distributions for all aerosol components), once per
150 minute. All AMS data were analysed using software packages SQUIRREL (v1.57I) and PIKA (v1.16I), available at
151 <http://cires1.colorado.edu/jimenez-group/ToFAMSResources/ToFSoftware/>.

152 The aerodynamic lens on the AMS has a transmission efficiency of nearly 100% for particles with
153 aerodynamic diameters of 70-500 nm; for somewhat smaller particles (30-70 nm), this transmission is lower but not
154 negligible (Jimenez et al., 2003). Thus, high enough solution concentrations are used such that the dried particles
155 formed in the nebulizer are larger than ~100 nm aerodynamic diameter. Collection efficiencies (CE) in the AMS can
156 vary depending on the extent to which aerosol particles bounce off the thermal element prior to vaporization. This
157 can impact the absolute concentrations observed, but for internally mixed samples, the relative concentrations of
158 different aerosol components are independent of CE. In this work, most measurements (including elemental ratios)
159 are reported as relative measurements, and thus no CE correction is applied. Some biases may arise if the aerosol is
160 not internally mixed, but for all systems examined so far in PToF, no size-dependence in composition was observed
161 (Figure S1).

162 **2.3 Sample Collection and Solution Preparation**

163 As described below, samples were prepared from a number of sources, including commercially available
164 standards, the extracts of chamber and ambient aerosol particles collected on filters, and dissolved organic matter from
165 the Pacific Ocean. For all solutions, either ultrapure water (18.2 M Ω cm, MilliQ) or HPLC-grade methanol was used.
166 Prior to use, all glassware was cleaned with a methanol solvent wash and baked at 450°C for 6 hours.

167 Chamber aerosol (enabling offline vs. online comparisons) was generated in the MIT 7.5-m³ Teflon
168 environmental chamber. Details on the facility are given elsewhere (Hunter et al., 2014). Experiments were run at 20
169 °C, < 5% RH, in the dark, and under low-NO_x conditions using ozone as the oxidant. Ammonium sulfate seeds were
170 added to a concentration of ~60 $\mu\text{g}/\text{m}^3$. The VOC, α -pinene, had an initial mixing ratio of 100 ppb; a penray lamp
171 (Jelight model 600) was used to add ~500 ppb ozone. Filter samples were collected on Zeflour® PTFE Membrane
172 Filters (0.5 μm pore size) at flow rates of ~5 L/min for 10 hr. Laboratory blank filters were prepared by placing
173 separate filters in the filter holder for 10 minutes before the start of the experiments. All filters were stored in baked
174 aluminum foil packets, sealed in plastic bags, and placed in a freezer at -20 °C until extraction. Filters were extracted
175 with ~4 mL of HPLC-grade methanol. In order to avoid oxidation of the organic species in the extract, no sonication
176 was used; instead, the vials were gently agitated by hand intermittently over 3 hours. Solutions were concentrated by
177 evaporating to dryness under a gentle stream of ultra-high purity N₂. Dried samples were stored in the freezer at -20



178 °C until reconstitution with MilliQ water and analysis by the SVN-AMS. Blank subtraction was carried out with a
179 scaling of the filter blank to 12% of the sample signal, as determined from the internal standard in each sample.

180 Field samples from the Southern Oxidant and Aerosol Study (SOAS) in 2013 were collected on pre-baked
181 Tissuquartz™ Filters (Pall Life Science, 8 x 10 in) at Look Rock, TN starting on 06/16/2013 using a high-volume
182 aerosol filter sampler with a PM_{2.5} cyclone (Tisch Environmental, Inc.) as described by Budisulistiorini et al. (2015).
183 For filter extraction, a 37 mm punch was extracted in a pre-cleaned scintillation vials with 20 mL high-purity methanol
184 (LC-MS Chromasolv-grade®, Sigma Aldrich) by sonication for 45 min. Filter extract was filtered through 0.2 µm
185 syringe filter (Acrodisc® PTFE membrane, Pall Life Sciences) to remove suspended filter fibers. The filtered extract
186 was then blown down to dryness under a gentle N_{2(g)} stream at room temperature. An aerosol chemical speciation
187 monitor (ACSM) (Ng et al., 2011a) was deployed at the same field site (Budisulistiorini et al., 2015); the average mass
188 spectrum for the length of the filter sample was used for comparison with the present SVN-AMS measurements.

189 Standard solutions were prepared from commercially available compounds dissolved in MilliQ water.
190 Reagents used included ammonium sulfate, ammonium nitrate, isotopically-labelled ammonium nitrate (NH₄¹⁵NO₃),
191 citric acid, mannitol, PEG-400, 4-hydroxy-3-methoxy-DL-mandelic acid (HMMA), and HPLC grade methanol, all
192 from Sigma-Aldrich.

193 The DOM was collected at the Natural Energy Laboratory Hawaii Authority facility in Kona, Hawaii.
194 Seawater from a depth of 20 m was pumped through a 0.2 µm filter to remove particles and the high molecular weight
195 fraction of organic matter in the filtrate was concentrated by ultrafiltration using a membrane with a 1 nm pore size
196 and a nominal 1,000 Dalton molecular weight cut off. This fraction was desalted by serial dilution/concentration with
197 MilliQ water and then freeze-dried. Low-molecular weight humic substances and residual salts were removed by
198 stirring with anion (hydroxide form) and cation exchange resins (hydrogen form). The final product was freeze-dried
199 to yield a fluffy white powder. Conventional CHNS analysis was carried out using a CE-440 Elemental Analyzer
200 (Exeter Analytical).

201 **3 Results and Discussion**

202 **3.1 Nebulization and Aerosol Size**

203 Figure 2a shows a time series of measured aerosol mass concentrations of a typical nebulized aerosol pulse
204 from a 4 µL solution containing approximately 0.33 g/L each of mannitol, ammonium sulfate, and ammonium nitrate.
205 The nebulizer is turned on at t = 0 and shortly afterwards (t = ~10 s) the aerosol packet is observed in the AMS. The
206 start of the nebulization is timed so that a closed (background) measurement occurs during the downslope of the signal
207 (t = ~16-21 s, dashed lines). This background is subtracted from the aerosol particle signal during data processing.
208 Measurements are collected until the signal returns to the baseline (t = ~44 s).

209 Figure 2b shows the size distribution of the particles generated by nebulizing an aqueous solution of citric
210 acid with continuous injection via syringe pump and a total concentration of ~1 g/L into an SMPS (TSI). The particles
211 have size distributions centered at 150-200 nm. We find injections of solutions with total concentrations above 0.2
212 g/L provide sufficient aerosol mass for analysis (Figure S1). These measurements compare well with calculations



213 based on the size of droplets reported by the manufacturer (Sonaer inc.) of approximately 1.7 μm using water solutions.
214 Assuming that the density of the dried particle is 1.3 g/cm^3 (Nakao et al., 2013), the minimum sample concentration
215 that will form a 100 nm dried particle is approximately 0.3 g/L . To generate large enough aerosol particles from more
216 dilute solutions, larger initial droplets could be formed by changing the piezo to a transducer that vibrates at a lower
217 frequency. However, for these larger droplets, drying will require the loss of a greater amount of solvent, so that any
218 impurities in the solvent will make up a larger (and possibly even dominant) fraction of the resulting fine particles.
219 Thus the use of ultrasonic nebulization at lower frequencies was not investigated here.

220

221 3.2 Quantification

222 3.2.1 Nebulization Efficiency

223 A key quantity describing the potential sensitivity of the SVN-AMS is the SVN nebulization efficiency, the
224 ratio of the mass measured in the AMS compared to the mass of analyte placed on the thin film. This was determined
225 by loading 4 μL of a known solution onto the film and measuring the mass of each component in the AMS integrated
226 over the injection pulse, determined by:

$$227 \quad M_{AMS} = \int_{t_1}^{t_2} f(t) dt \times v_{AMS}$$

228 where M_{AMS} is the mass measured by the AMS in μg , $f(t)$ is the instantaneous mass concentration measured in the
229 AMS ($\mu\text{g}/\text{m}^3$), and v_{ams} , is the gas flow rate into the AMS in m^3/s . For each injection, the background-subtracted AMS
230 signal is calculated (Figure 2a). The gaps due to closed cycles are bridged by interpolation and the area under the
231 injection curve is calculated via trapezoidal integration from time points before and after the pulse (t_1 and t_2 ,
232 respectively) with the time steps (dt) corresponding to the MS cycle time (here 0.5 s). The mass measured in the AMS
233 is affected by three factors: the amount of aerosol formed and transported out of the SVN, the fraction of the gas flow
234 from the SVN that is sampled by the AMS (typically $\sim 1/2$), and the fraction of aerosol that bounces off the heater
235 element before vaporizing (the AMS CE).

236 Figure 3 shows the mass measured in the AMS compared to the mass deposited on the nebulizer for replicate
237 injections of four different aqueous solutions of citric acid, ammonium nitrate, ammonium sulfate, and isotopically-
238 labeled ammonium nitrate ($\text{NH}_4^{15}\text{NO}_3$, used later as an internal standard) with concentrations ranging between
239 approximately 0.1 and 0.2 g/L for each of the components (but with the same total concentration, 0.75 g/L). The
240 amount of mass measured in the AMS increases slowly compared to the amount placed on the film, and variations in
241 measured masses are observed for replicate injections of the same sample. The observed increase in the mass
242 measured for these samples is likely partially related to CE on the vaporizer, as the highest efficiency was observed
243 for samples with the largest mass fractions of organic. The measured nebulization efficiencies are on the order of
244 0.02-0.06%, indicating that the aerosol mass detected with the AMS is approximately three orders of magnitude lower
245 than the mass originally deposited on the thin film.

246 The majority of the sample mass loss likely occurs during the nebulization process itself. For aqueous
247 solutions in the SVN, large droplets are observed to be ejected off the surface of the film at the same time as the
248 aerosol is generated. These ejected droplets are then lost to the walls of the SVN. The ejection of these droplets



249 appears to be a necessary part of the nebulization mechanism for water samples as smaller volumes ($< 1 \mu\text{L}$) of water
250 do not generate such droplets and also do not appear to form aerosol. This observed mechanism is in agreement with
251 previous studies of aerosol generation for ultrasonic nebulization, in which cavitation within the droplet (Lang, 1962)
252 and boiling and/or jetting from a droplet chain (Simon et al., 2015) have been observed.

253 The size distribution and number of aerosol particles from ultrasonic nebulization have been shown to be
254 affected by the frequency of the ultrasonic vibration, the properties of the liquid including surface tension, density,
255 and viscosity, and the concentration of the solution (Donnelly et al., 2005; Lang, 1962; Simon et al., 2015). The present
256 application involves relatively dilute solution, so the only parameter that could be varied was the surface tension, by
257 use of different solvents. Nebulization of solvents with lower surface tension, such as methanol, led to the ejection of
258 much smaller droplets, and consequently substantially higher nebulization efficiencies ($\sim 10\%$). However, methanol
259 (and other HPLC-grade organic solvents) was found to give higher background signals in the AMS than MilliQ water,
260 likely due to higher levels of low-volatility contaminants. This difference was also observed by Daellenbach *et al.*
261 (2016); therefore, MilliQ water appears to be the ideal solvent to use for most environmental samples. However, with
262 adequate solvent background characterization, organic solvents may be optimal for environmental samples with more
263 non-polar components (e.g. petroleum or fresh tail pipe emissions).

264 3.2.2 Internal Standards and Calibration Curves

265 In Figure 3, the vertical spread of data points shows the variation in nebulization efficiency from one injection
266 to the next. This is likely the result of small differences in the droplet shape or position on the film, leading to
267 differences in how the droplets are ejected from the surface during aerosol formation. This run-to-run variability in
268 nebulization efficiency, as well as the lack of a linear correlation between the mass placed on the film and the mass
269 observed, complicates quantification, and necessitates the use of an internal standard to quantify the concentration of
270 organic species within the original sample. In some cases, an inorganic ion that is independently quantified, such as
271 sulfate, can serve as this internal standard (Daellenbach et al., 2016). However, in many cases such an independent
272 measurement is not available; additionally, some environmental samples may not contain appreciable levels of
273 measurable inorganic species, or else such species may not be soluble in the solvent of choice (e.g. ionic species in
274 organic solvents). In these cases, an internal standard needs to be added to the solution prior to nebulization.

275 For use with the AMS, the internal standard must meet a number of requirements: it must be non-refractory,
276 soluble, unreactive with the other sample components, not already present in the solution, and easily distinguishable
277 from other species in the sample. For nebulization of samples dissolved in organic solvents, organic internal standards
278 (e.g., phthalic acid (Chen et al., 2016; Han et al., 2016)) meet these requirements. In the present work, which focuses
279 on aqueous samples only, we use an inorganic internal standard of isotopically-labelled ammonium nitrate
280 ($\text{NH}_4^{15}\text{NO}_3$). An example mass spectrum for an internal standard solution is shown in Figure 4a. The background
281 signal from other components (organic, sulfate, and nitrate) is very low. Another tested option is ammonium iodide
282 (NH_4I). Both of these salts work well as internal standards for both laboratory and ambient samples, since neither
283 $^{15}\text{NO}_3$ nor iodide are present in appreciable amounts in the atmosphere and there is usually a very small contribution



284 of organic fragments at the fragment masses observed for those salts. The internal standards are added at the same
285 order of magnitude concentration as the sample.

286 Figure 4b shows calibration curves with linear responses for three different organic compounds (citric acid,
287 4-hydroxy-3-methoxy-DL-mandelic acid (HMMA), and polyethylene glycol 400 (PEG-400)) at four concentrations
288 using $\text{NH}_4^{15}\text{NO}_3$ as the internal standard. For the calibration curve, the ratios of the AMS signals for the analyte over
289 the internal standard are compared to the ratios for known solution concentrations, thus correcting any variations in
290 the mass of analyte nebulized. For quantification of unknowns, known concentrations of the internal standard are
291 added to the samples. The ratio of the measured AMS signals can then be used to calculate the unknown analyte
292 concentration from the calibration curve.

293 For quantification of complex organic mixtures using this technique, the most accurate organic calibration
294 standards will have chemical structures similar to the average structure of the mixture. The slope of each line is related
295 to the relative ionization efficiency (RIE) of the organic compound in the AMS (Jimenez et al., 2003). The RIE values
296 in Figure 4b for HMMA and citric acid (1.01 and 1.95, respectively) bracket the range of RIE values for different
297 types of organics measured using standard AMS calibration techniques (Jimenez et al., 2016). This range likely arises
298 from differences in how the organic compounds dissociate during volatilization on the heater. The heater in the AMS
299 is typically set at 600°C, and so most organic molecules found in organic aerosol thermally decompose prior to electron
300 impact ionization (Canagaratna et al., 2015) leading to RIEs in the range of 1.0-2.0. In contrast, the slope of 2.62 for
301 PEG-400 is substantially outside of the range of values. However, with the AMS, complex mixtures are less likely to
302 show large variations in RIE than different individual compounds, such as those used in Figure 4. For extracts of
303 atmospheric aerosol or other smaller organic mixtures, the RIE of 1.4, which is typically used for AMS measurements
304 (Canagaratna et al., 2007; Jimenez et al., 2016; Xu et al., 2018), is likely the best value to use. For extracts of other
305 types of organic mixtures, compounds that have a structure similar to the average organic composition should be used
306 to calibrate the samples.

307 3.1 Mass Spectral Analysis

308 The primary goal of the SVN-AMS is to measure quantitative chemical information, specifically elemental
309 ratios, from complex organic mixtures. We have characterized these for a number of different chemical systems,
310 described below. Results are summarized in Figure 5 (comparing SVN-AMS and online AMS mass spectra) and Table
311 1 (comparing elemental ratios measured with SVN-AMS with those measured by either online AMS or CHNS
312 analysis).

313 One concern with using ultrasonic nebulization to generate aerosol particles is the possibility that the high
314 temperatures possibly reached by the solution during nebulization may degrade the organic compounds, affecting their
315 mass spectra (and hence measured elemental composition). Figure 5a shows a comparison of a solution containing 1
316 g/L citric acid aerosolized with a TSI atomizer (black) and the SVN (green), with the inset showing a direct comparison
317 between the intensities measured for each ion in the mass spectrum. The degree of agreement can be described by the
318 dot product of the two spectra, as well as the log of the intensities before taking the dot product (log-dot product),
319 which gives the lower intensity peaks greater weight. Very good overlap between the two mass spectra is observed,



320 with a dot product of 0.99 and a log-dot product of 0.96. This indicates minimal degradation of the citric acid by
321 ultrasonic nebulization.

322 A high degree of similarity is also observed between offline and online aerosol measurements for more
323 complex mixtures. Figure 5b shows mass spectra for a comparison of offline (red) vs. online (black) SOA sample,
324 generated from the dark ozonolysis of α -pinene. For all filter samples, spectra from the SVN are background
325 subtracted using spectra collected from blank filter samples. The overlap in Figure 5b between the mass spectra is
326 very good, with a dot product of 0.98 and a log-dot product of 0.98. The elemental ratios are also very similar between
327 the two samples with an H:C of 1.6 for both and O:C of 0.48 for the chamber and 0.49 for the SVN samples (Table
328 1). The largest difference is observed at m/z 44 (CO_2^+) and m/z 43 ($\text{C}_2\text{H}_3\text{O}^+$) with a larger fraction of CO_2^+ in the
329 offline sample. The intensity of CO^+ (m/z 28) is also different, but only because it is set equal to the intensity of the
330 CO_2^+ ion, as is commonly done for ambient sampling with the AMS (given that the CO^+ ion generally cannot be
331 distinguished from the much more abundant N_2^+ ion (Aiken et al., 2007). The organic contribution from H_2O^+ , OH^+ ,
332 and O^+ is also constrained by the CO_2^+ signal so any differences in CO_2^+ intensity will also show up in those ions
333 (Aiken et al., 2008). The observed difference in CO_2^+ and $\text{C}_2\text{H}_3\text{O}^+$ ion intensity is likely a result of the extraction step
334 prior to nebulization, which may preferentially dissolve the most water-soluble (oxidized) SOA components; however,
335 based on the agreement in H:C and O:C in the online and offline cases, this does not appear to bias elemental ratio
336 measurements substantially.

337 Figure 5c shows a comparison of online and offline measurements of ambient organic aerosol, specifically
338 ACSM measurements and SVN-AMS measurements of a filter extract collected simultaneously during the 2013
339 SOAS field campaign in Look Rock, TN (8 pm July 4 to 7am July 5, 2013; EST). Since the ACSM is a unit-mass-
340 resolution instrument, the HR-AMS data are degraded to unit mass resolution, and ions that are determined from the
341 m/z 44 signal ($m/z=15, 16, 17, 18, \text{ and } 28$) are excluded from the analysis. Additionally, ions at m/z 30 and 31 were
342 removed from comparison because of interferences from the internal standard (m/z 31) and nitrate in the sample (m/z
343 30).

344 The two mass spectra in Figure 5c have a high degree of agreement between the major ions (dot product of
345 0.98). However, there is substantially more variation between the two techniques than in the chamber study, especially
346 in the lower-abundance peaks ($m/z>45$; see inset), as reflected in the lower log-dot product of only 0.90. Possible
347 reasons for this lower correlation include fractionation from the extraction step, the different sizes measured ($\text{PM}_{2.5}$
348 for the filter vs. PM_1 for the ACSM) (Daellenbach et al., 2016), the uncertainty in ACSM signals at higher masses due
349 to uncertainty in the relative ion transmission curve (Ng et al., 2011a), and/or the losses of more volatile compounds
350 during collection, extraction, and handling. Additional work is necessary to quantify the importance of these effects.
351 Regardless, the high degree of overlap between the online (AMS/ACSM) measurements and offline (SVN-AMS)
352 results indicates that the ensemble organic composition for these aerosol samples is generally well-represented by the
353 SVN-AMS measurements (Table 1).

354 For the SVN, the small sample volume requirements can make it attractive for the analysis of other
355 environmental samples that are soluble in water (or organic solvents) and that have low enough vapor pressures to
356 remain in the condensed phase after nebulization. Figure 3d shows an example AMS mass spectrum from dissolved



357 organic matter (DOM) from the Pacific Ocean. The mass spectrum is dominated by oxidized fragments containing
358 one or more oxygen atoms with smaller amounts of nitrogen-containing fragments. The measured N:C and H:C values
359 of 0.081 and 1.7, respectively, matches those measured by CHNS analysis (0.080 and 1.74, respectively). This
360 demonstrates that with the SVN, microgram quantities of dissolved environmental mixtures can be nebulized and
361 sampled into the AMS providing a rapid, quantitative method to determine elemental ratios in these complex organic
362 mixtures.

363 **4 Conclusions**

364 A new ultrasonic nebulizer has been described and characterized for generation of aerosol from very small
365 sample masses. We demonstrate the application of this technique to offline AMS analysis of complex organic
366 mixtures from aerosol filter extracts and DOM. Data sets that include quantitative organic mass, characteristic mass
367 spectra, and quantitative elemental ratios can be generated from only 0.4-1.2 μg of material. A direct comparison
368 between the mass spectra generated by commercial spray atomizers or by real-time aerosol particles sampled directly
369 from the atmosphere showed high degrees of agreement. Nebulization of aqueous samples generated measurable
370 aerosol from 0.1% of the sample mass. Higher nebulization efficiencies (and smaller ejected droplets) were observed
371 for methanol, likely due to its lower surface tension. The SVN, combined with offline-AMS, provides rapid analysis
372 of non-refractory organic and inorganic compounds. For other types of characterization, including analysis of
373 refractory material or organic molecular composition, the SVN can also be coupled with other aerosol instrumentation
374 such as PALMS or CIMS instruments.

375 Future improvements in the nebulization and collection efficiency of the SVN-AMS will enable analysis with
376 even lower sample mass requirements. The use of organic internal standards is one method to potentially improve
377 collection efficiency in the AMS. Additionally, the use of solvents with lower surface tension than water shows
378 promise for improved nebulization efficiencies. A useful future direction for this technique will be to characterize the
379 background signal in different organic solvents and optimize the continuous flow configuration to minimize the return
380 of large ejected droplets back onto the film. Continuous flow with organic solutions will also enable the analysis of
381 more hydrophobic organic samples such as fresh vehicle emissions, cooking oils, and petrochemical samples. In the
382 future, the SVN can be used to generate aerosol for analysis of other environmental samples to investigate sources or
383 processing/aging of these organic mixtures. The SVN, combined with aerosol measurement techniques such as the
384 AMS, provides a rapid, quantitative method to characterize the chemical and elemental properties of complex organic
385 mixtures, producing rich data sets for the exploration of exceptionally trace environmental samples.

386

387

388

389

390

391

392



393 **Supporting Information**

394 The supporting information is available free of charge at DOI:xxx. The document contains additional information on
395 particle sizes and memory effects between runs, (file type, PDF).

396 **Corresponding Author**

397 Rachel E. O'Brien, College of William and Mary, reobrien@wm.edu.

398 **Author Contributions**

399 MRC, JTJ, PLC, DRW, JHK, and KJR designed and built the SVN. SHB, JDS, CLF, DJR provided ambient aerosol
400 samples and DOM. REO and JHK designed experiments and REO carried them out. REO prepared the manuscript
401 with contributions from all authors.

402 **Data availability**

403 All data sets including mass spectra and SMPS data are available on request from REO, reobrien@wm.edu.

404 **Acknowledgement**

405 This work was supported by National Oceanic and Atmospheric Administration Grants No. NA13OAR4310072 and
406 NA14OAR4310132. KJB acknowledges support from the National Science Foundation. SHB and JDS acknowledges
407 support from the US Environmental Protection Agency Award No. 835404, Electric Power Research Institute (EPRI),
408 and National Oceanic and Atmospheric Administration Grant No. NA13OAR4310064. Special thanks to Dr. David
409 Karl and Mr. Eric Grabowski, University of Hawaii, for the CHNS elemental analysis of DOM. DJR acknowledges
410 support from the Gordan and Betty Moore Foundation award 6000 and the Simons Foundation SCOPE award 329108.

411 **References**

412 Aiken, A. C., DeCarlo, P. F. and Jimenez, J. L.: Elemental analysis of organic species with electron ionization high-
413 resolution mass spectrometry, *Anal. Chem.*, 79(21), 8350–8358, doi:10.1021/ac071150w, 2007.

414 Aiken, A. C., Decarlo, P. F., Kroll, J. H., Worsnop, D. R., Huffman, J. A., Docherty, K. S., Ulbrich, I. M., Mohr, C.,
415 Kimmel, J. R., Sueper, D., Sun, Y., Zhang, Q., Trimborn, A., Northway, M., Ziemann, P. J., Canagaratna, M. R.,
416 Onasch, T. B., Alfarra, M. R., Prevot, A. S. H., Dommen, J., Duplissy, J., Metzger, A., Balensperger, U. and Jimenez,
417 J. L.: O/C and OM/OC Ratios of Primary, Secondary, and Ambient Organic Aerosols with High-Resolution Time-of-
418 Flight Aerosol Mass Spectrometry, *Environ. Sci. Technol.*, 42, 4478–4485, doi:10.1021/es703009q, 2008.

419 Becker, J. W., Berube, P. M., Follett, C. L., Waterbury, J. B., Chisholm, S. W., Delong, E. F., Repeta, D. J. and Metz,



- 420 T.: Closely related phytoplankton species produce similar suites of dissolved organic matter, *Front. Microbiol.*, 5(111),
421 1–14, doi:10.3389/fmicb.2014.00111, 2014.
- 422 Bozzetti, C., Daellenbach, K. R., Hueglin, C., Fermo, P., Sciare, J., Kasper-Giebl, A., Mazar, Y., Abbaszade, L., El
423 Kazzi, M., Gonzalez, R., Shuster-Meiseles, T., Flasch, M., Wolf, R., Kr, A., Francesco Canonaco, E., Schnelle-Kreis,
424 R., Slowik, J. G., Zimmermann, R., Rudich, Y., Baltensperger, U., El Haddad, I. and Preo, A. H.: Size-Resolved
425 Identification, Characterization, and Quantification of Primary Biological Organic Aerosol at a European Rural Site,
426 *Environ. Sci. Technol.*, 50, 3425–3434, doi:10.1021/acs.est.5b05960, 2016.
- 427 Bozzetti, C., Sosedova, Y., Xiao, M., Daellenbach, K. R., Ulevicius, V., Dudoitis, V., Mordas, G., Byčenkienė, E. S.
428 E., Plauškaitė, K., Vlachou, A., Golly, B., Chazéau, B., Besombes, J.-L., Baltensperger, U., Jaffrezo, J.-L., Slowik,
429 J. G., Haddad, I. El and Prévôt, A. S. H.: Argon offline-AMS source apportionment of organic aerosol over yearly
430 cycles for an urban, rural, and marine site in northern Europe, *Atmos. Chem. Phys.*, 17, 117–141, doi:10.5194/acp-17-
431 117-2017, 2017.
- 432 Budisulistiorini, S. H., Li, X., Bairai, S. T., Renfro, J., Liu, Y., Liu, Y. J., McKinney, K. A., Martin, S. T., McNeill, V.
433 F., Pye, H. O. T., Nenes, A., Neff, M. E., Stone, E. A., Mueller, S., Knote, C., Shaw, S. L., Zhang, Z., Gold, A. and
434 Surratt, J. D.: Examining the effects of anthropogenic emissions on isoprene-derived secondary organic aerosol
435 formation during the 2013 Southern Oxidant and Aerosol Study (SOAS) at the Look Rock, Tennessee ground site,
436 *Atmos. Chem. Phys.*, 15, 8871–8888, doi:10.5194/acp-15-8871-2015, 2015.
- 437 Canagaratna, M. R., Jayne, J. T., Jimenez, J. L., Allan, J. D., Alfarra, M. R., Zhang, Q., Onasch, T. B., Drewnick, F.,
438 Coe, H., Middlebrook, A., Delia, A., Williams, L. R., Trimborn, A. M., Northway, M. J., Decarlo, P. F., Kolb, C. E.,
439 Davidovits, P. and Worsnop, D. R.: Chemical and Microphysical Characterization of Ambient Aerosols with the
440 Aerodyne Aerosol Mass Spectrometer, *Mass Spec Rev.*, 26, 185–222, doi:10.1002/mas.20115, 2007.
- 441 Canagaratna, M. R., Jimenez, J. L., Kroll, J. H., Chen, Q., Kessler, S. H., Massoli, P., Hildebrandt Ruiz, L., Fortner,
442 E., Williams, L. R., Wilson, K. R., Surratt, J. D., Donahue, N. M., Jayne, J. T. and Worsnop, D. R.: Elemental ratio
443 measurements of organic compounds using aerosol mass spectrometry: characterization, improved calibration, and
444 implications, *Atmos. Chem. Phys.*, 15, 253–272, doi:10.5194/acp-15-253-2015, 2015.
- 445 Chen, Q., Heald, C. L., Jimenez, J. L., Canagaratna, M. R., Zhang, Q., He, L.-Y., Huang, X.-F., Campuzano-Jost, P.,
446 Palm, B. B., Poulain, L., Kuwata, M., Martin, S. T., Abbatt, J. P. D., Lee, A. K. Y. and Liggio, J.: Elemental
447 composition of organic aerosol: The gap between ambient and laboratory measurements, *Geophys. Res. Lett.*, 42(10),
448 4182–4189, doi:10.1002/2015GL063693, 2015.
- 449 Chen, Q., Ikemori, F. and Mochida, M.: Light Absorption and Excitation–Emission Fluorescence of Urban Organic
450 Aerosol Components and Their Relationship to Chemical Structure, *Environ. Sci. Technol.*, 50, 10859–10868,
451 doi:10.1021/acs.est.6b02541, 2016.
- 452 Daellenbach, K. R., Bozzetti, C., Křepelová, A., Canonaco, F., Wolf, R., Zotter, P., Fermo, P., Crippa, M., Slowik, J.
453 G., Sosedova, Y., Zhang, Y., Huang, R. J., Poulain, L., Szidat, S., Baltensperger, U., El Haddad, I. and Prévôt, A. S.



- 454 H.: Characterization and source apportionment of organic aerosol using offline aerosol mass spectrometry, *Atmos.*
455 *Meas. Tech.*, 9(1), 23–39, doi:10.5194/amt-9-23-2016, 2016.
- 456 Daumit, K. E., Kessler, S. H. and Kroll, J. H.: Average chemical properties and potential formation pathways of highly
457 oxidized organic aerosol, *Faraday Discuss.*, 165, 181–201, doi:10.1039/c3fd00045a, 2013.
- 458 Decarlo, P. F., Kimmel, J. R., Trimborn, A., Northway, M. J., Jayne, J. T., Aiken, A. C., Gonin, M., Fuhrer, K.,
459 Horvath, T., Docherty, K. S., Worsnop, D. R. and Jimenez, J. L.: Field-Deployable, High-Resolution, Time-of-Flight
460 Aerosol Mass Spectrometer, *Anal. Chem.*, 78(24), 8281–8289, doi:10.1029/2001JD001213, *Analytical*, 2006.
- 461 Donnelly, T. D., Hogan, J., Mugler, A., Schubmehl, M., Schommer, N., Bernoff, A. J., Dasnurkar, S. and Ditmire, T.:
462 Using ultrasonic atomization to produce an aerosol of micron-scale particles, *Rev. Sci. Instrum.*, 76(11), 1–10,
463 doi:10.1063/1.2130336, 2005.
- 464 Gallimore, P. J. and Kalberer, M.: Characterizing an Extractive Electrospray Ionization (EESI) Source for the Online
465 Mass Spectrometry Analysis of Organic Aerosols, *Environ. Sci. Technol.*, (47), 734–7331, doi:10.1021/es305199h,
466 2013.
- 467 Ge, X., Li, L., Chen, Y., Chen, H., Wu, D., Wang, J., Xie, X., Ge, S., Ye, Z., Xu, J. and Chen, M.: Aerosol
468 characteristics and sources in Yangzhou, China resolved by offline aerosol mass spectrometry and other techniques,
469 *Environ. Pollut.*, 225, 74–85, doi:10.1016/j.envpol.2017.03.044, 2017.
- 470 Han, Y., Kawamura, K., Chen, Q. and Mochida, M.: Formation of high-molecular-weight compounds via the
471 heterogeneous reactions of gaseous C8–C10 n-aldehydes in the presence of atmospheric aerosol components, *Atmos.*
472 *Environ.*, 126, 290–297, doi:10.1016/j.atmosenv.2015.11.050, 2016.
- 473 Hansman, R. L., Dittmar, T. and Herndl, G. J.: Conservation of dissolved organic matter molecular composition during
474 mixing of the deep water masses of the northeast Atlantic Ocean, *Mar. Chem.*, 177, 288–297,
475 doi:10.1016/j.marchem.2015.06.001, 2015.
- 476 Heald, C. L., Kroll, J. H., Jimenez, J. L., Docherty, K. S., Decarlo, P. F., Aiken, A. C., Chen, Q., Martin, S. T., Farmer,
477 D. K. and Artaxo, P.: A simplified description of the evolution of organic aerosol composition in the atmosphere,
478 *Geophys. Res. Lett.*, 37(L08803), 1–5, doi:10.1029/2010GL042737, 2010.
- 479 Huang, R.-J., Zhang, Y., Bozzetti, C., Ho, K.-F., Cao, J.-J., Han, Y., Daellenbach, K. R., Slowik, J. G., Platt, S. M.,
480 Canonaco, F., Zotter, P., Wolf, R., Pieber, S. M., Bruns, E. A., Crippa, M., Ciarelli, G., Piazzalunga, A., Schwikowski,
481 M., Abbaszade, G., Schnelle-Kreis, J., Zimmermann, R., An, Z., Szidat, S., Baltensperger, U., Haddad, I. El and
482 Prévôt, A. S. H.: High secondary aerosol contribution to particulate pollution during haze events in China, *Nature*,
483 514, doi:10.1038/nature13774, 2014.
- 484 Hunter, J. F., Carrasquillo, A. J., Daumit, K. E. and Kroll, J. H.: Secondary Organic Aerosol Formation from Acyclic,
485 Monocyclic, and Polycyclic Alkanes, *Environ. Sci. Technol.*, 48, 10227–10234, doi:10.1021/es502674s, 2014.



- 486 Jimenez, J. L., Jayne, J. T., Shi, Q., Kolb, C. E., Worsnop, D. R., Yourshaw, I., Seinfeld, J. H., Flagan, R. C., Zhang,
487 X., Smith, K. A., Morris, J. W. and Davidovits, P.: Ambient aerosol sampling using the Aerodyne Aerosol Mass
488 Spectrometer, *J. Geophys. Res.*, 108, 8425, doi:10.1029/2001JD001213, 2003.
- 489 Jimenez, J. L., Canagaratna, M. R., Donahue, N. M., Prevot, A. S. H., Zhang, Q., Kroll, J. H., Decarlo, P. F., Allan, J.
490 D., Coe, H., Ng, N. L., Aiken, A. C., Docherty, K. S., Ulbrich, I. M., Grieshop, A. P., Robinson, A. L., Duplissy, J.,
491 Smith, J. D., Wilson, K. R., Lanz, V. A., Hueglin, C., Sun, Y. L., Tian, J., Laaksonen, A., Raatikainen, T., Rautiainen,
492 J., Vaattovaara, P., Ehn, M., Kulmala, M., Tomlinson, J. M., Collins, D. R., Cubison, M. J., Dunlea, E. J., Huffman,
493 J. A., Onasch, T. B., Alfarra, M. R., Williams, P. I., Bower, K., Kondo, Y., Schneider, J., Drewnick, F., Borrmann, S.,
494 Weimer, S., Demerjian, K., Salcedo, D., Cottrell, L., Griffin, R., Takami, A., Miyoshi, T., Hatakeyama, S., Shimono,
495 A., Sun, J. Y., Zhang, Y. M., Dzepina, K., Kimmel, J. R., Sueper, D., Jayne, J. T., Herndon, S. C., Trimborn, A. M.,
496 Williams, L. R., Wood, E. C., Middlebrook, A. M., Kolb, C. E., Baltensperger, U. and Worsnop, D. R.: Evolution of
497 Organic Aerosols in the Atmosphere, *Science* (80-.), 326, 1525–1529, doi:10.1126/science.1179518, 2009.
- 498 Jimenez, J. L., Canagaratna, M. R., Drewnick, F., Allan, J. D., Alfarra, M. R., Middlebrook, A. M., Slowik, J. G.,
499 Zhang, Q., Coe, H., Jayne, J. T. and Worsnop, D. R.: Comment on “The effects of molecular weight and thermal
500 decomposition on the sensitivity of a thermal desorption aerosol mass spectrometer,” *Aerosol Sci. Technol.*, 50, i–xv,
501 doi:10.1080/02786826.2016.1205728, 2016.
- 502 Kaul, D. S., Gupta, T. and Tripathi, S. N.: Source Apportionment for Water Soluble Organic Matter of Submicron
503 Aerosol: A Comparison between Foggy and Nonfoggy Episodes, *Aerosol Air Qual. Res.*, 14, 1527–1533,
504 doi:10.4209/aaqr.2013.10.0319, 2014.
- 505 Kimmel, J. R., Farmer, D. K., Cubison, M. J., Sueper, D., Tanner, C., Nemitz, E., Worsnop, D. R., Gonin, M. and
506 Jimenez, J. L.: Real-time aerosol mass spectrometry with millisecond resolution, *Int. J. Mass Spectrom.*, 303, 15–26,
507 doi:10.1016/j.ijms.2010.12.004, 2010.
- 508 Koch, B. P., Witt, M., Engbrodt, R., Dittmar, T. and Kattner, G.: Molecular formulae of marine and terrigenous
509 dissolved organic matter detected by electrospray ionization Fourier transform ion cyclotron resonance mass
510 spectrometry, *Geochim. Cosmochim. Acta*, 69(13), 3299–3308, doi:10.1016/j.gca.2005.02.027, 2005.
- 511 Kroll, J. H., Donahue, N. M., Jimenez, J. L., Kessler, S. H., Canagaratna, M. R., Wilson, K. R., Altieri, K. E.,
512 Mazzoleni, L. R., Wozniak, A. S., Bluhm, H., Mysak, E. R., Smith, J. D. and Kolb, C. E.: Carbon oxidation state as a
513 metric for describing the chemistry of atmospheric organic aerosol, *Nat. Chem.*, 3, 133–139,
514 doi:10.1038/NCHEM.948, 2011.
- 515 Kroll, J. H., Lim, C. Y., Kessler, S. H. and Wilson, K. R.: Heterogeneous Oxidation of Atmospheric Organic Aerosol:
516 Kinetics of Changes to the Amount and Oxidation State of Particle-Phase Organic Carbon, *J. Phys. Chem. A*, 119,
517 10767–10783, doi:10.1021/acs.jpca.5b06946, 2015.
- 518 Lang, R. J.: Ultrasonic Atomization of Liquids, *J. Acoust. Soc. Am.*, 34(1), 6–8, 1962.



- 519 Lee, A. K. Y., Hayden, K. L., Herckes, P., Leaitch, W. R., Liggio, J., Macdonald, A. M. and Abbatt, J. P. D.:
520 Characterization of aerosol and cloud water at a mountain site during WACS 2010: secondary organic aerosol
521 formation through oxidative cloud processing, *Atmos. Chem. Phys. Atmos. Chem. Phys.*, 12, 7103–7116,
522 doi:10.5194/acp-12-7103-2012, 2012.
- 523 Lopez-Hilfiker, F. D., Mohr, C., Ehn, M., Rubach, F., Kleist, E., Wildt, J., Mentel, T. F., Lutz, A., Hallquist, M.,
524 Worsnop, D. and Thornton, J. A.: A novel method for online analysis of gas and particle composition: description and
525 evaluation of a Filter Inlet for Gases and AEROSols (FIGAERO), *Atmos. Meas. Tech.*, 7, 983–1001, doi:10.5194/amt-
526 7-983-2014, 2014.
- 527 Lu, Y., Li, X., Mesfioui, R., Bauer, J. E., Chambers, R. M., Canuel, E. A. and Hatcher, P. G.: Use of ESI-FTICR-MS
528 to Characterize Dissolved Organic Matter in Headwater Streams Draining Forest-Dominated and Pasture-Dominated
529 Watersheds, *PLoS One*, 1–21, doi:10.1371/journal.pone.0145639, 2015.
- 530 Mihara, T. and Mochida, M.: Characterization of Solvent-Extractable Organics in Urban Aerosols Based on Mass
531 Spectrum Analysis and Hygroscopic Growth Measurement, *Environ. Sci. Technol.*, 45, 9168–9174,
532 doi:10.1021/es201271w, 2011.
- 533 Murphy, D. M., Thomson, D. S. and Mahoney, M. J.: In Situ Measurements of Organics, Meteoritic Material,
534 Mercury, and Other Elements in Aerosols at 5 to 19 Kilometers, *Science (80-.)*, 282, 1664–1669, 1998.
- 535 Nakao, S., Tang, P., Tang, X., Clark, C. H., Qi, L., Seo, E., Asa-Awuku, A. and Iii, D. C.: Density and elemental ratios
536 of secondary organic aerosol: Application of a density prediction method, *Atmos. Environ.*, 68, 273–277,
537 doi:10.1016/j.atmosenv.2012.11.006, 2013.
- 538 Ng, N. L., Herndon, S. C., Trimborn, a., Canagaratna, M. R., Croteau, P. L., Onasch, T. B., Sueper, D., Worsnop, D.
539 R., Zhang, Q., Sun, Y. L. and Jayne, J. T.: An Aerosol Chemical Speciation Monitor (ACSM) for Routine Monitoring
540 of the Composition and Mass Concentrations of Ambient Aerosol, *Aerosol Sci. Technol.*, 45(7), 780–794,
541 doi:10.1080/02786826.2011.560211, 2011a.
- 542 Ng, N. L., Canagaratna, M. R., Jimenez, J. L., Chhabra, P. S., Seinfeld, J. H. and Worsnop, D. R.: Changes in organic
543 aerosol composition with aging inferred from aerosol mass spectra, *Atmos. Chem. Phys. Atmos. Chem. Phys.*, 11,
544 6465–6474, doi:10.5194/acp-11-6465-2011, 2011b.
- 545 Simon, J. C., Sapozhnikov, O. A., Khokhlova, V. A., Crum, L. A. and Bailey, M. R.: Ultrasonic atomization of liquids
546 in drop-chain acoustic fountains, *J Fluid Mech.*, 766, 129–146, doi:10.1017/jfm.2015.11.Ultrasonic, 2015.
- 547 Skoog, D. F., Holler, F. J. and Nieman, T. A.: Principles of Instrumental Analysis, Saunders College Pub,
548 Philadelphia., 1998.
- 549 Sun, Y., Zhang, Q., Zheng, M., Ding, X., Edgerton, E. S. and Wang, X.: Characterization and Source Apportionment
550 of Water-Soluble Organic Matter in Atmospheric Fine Particles (PM 2.5) with High-Resolution Aerosol Mass
551 Spectrometry and GC-MS, *Environ. Sci. Technol.*, 45, 4854–4861, doi:10.1021/es200162h, 2011.



552 Xu, J., Zhang, Q., Li, X., Ge, X., Xiao, C., Ren, J. and Qin, D.: Dissolved Organic Matter and Inorganic Ions in a
553 Central Himalayan Glacier-Insights into Chemical Composition and Atmospheric Sources, *Environ. Sci. Technol.*,
554 47, 6181–6188, doi:10.1021/es4009882, 2013.

555 Xu, J. Z., Zhang, Q., Wang, Z. B., Yu, G. M., Ge, X. L. and Qin, X.: Chemical composition and size distribution of
556 summertime PM_{2.5} at a high altitude remote location in the northeast of the Qinghai-Xizang (Tibet) Plateau: Insights
557 into aerosol sources and processing in free troposphere, *Atmos. Chem. Phys.*, 15(9), 5069–5081, doi:10.5194/acp-15-
558 5069-2015, 2015.

559 Xu, W., Lambe, A., Silva, P., Hu, W., Onasch, T., Williams, L., Croteau, P., Zhang, X., Renbaum-Wolff, L., Fortner,
560 E., Jimenez, J. L., Jayne, J., Worsnop, D. and Canagaratna, M.: Laboratory evaluation of species-dependent relative
561 ionization efficiencies in the Aerodyne Aerosol Mass Spectrometer Laboratory evaluation of species-dependent
562 relative ionization efficiencies in the Aerodyne Laboratory eva, *Aerosol Sci. Technol.*, 52(6), 626–641,
563 doi:10.1080/02786826.2018.1439570, 2018.

564 Ye, Z., Liu, J., Gu, A., Feng, F., Liu, Y., Bi, C., Xu, J., Li, L., Chen, H., Chen, Y., Dai, L., Zhou, Q. and Ge, X.:
565 Chemical characterization of fine particulate matter in Changzhou, China, and source apportionment with offline
566 aerosol mass spectrometry, *Atmos. Chem. Phys.*, 17, 2573–2592, doi:10.5194/acp-17-2573-2017, 2017.

567

568

569

570

571

572

573

574

575

576

577 **Figures and Tables**

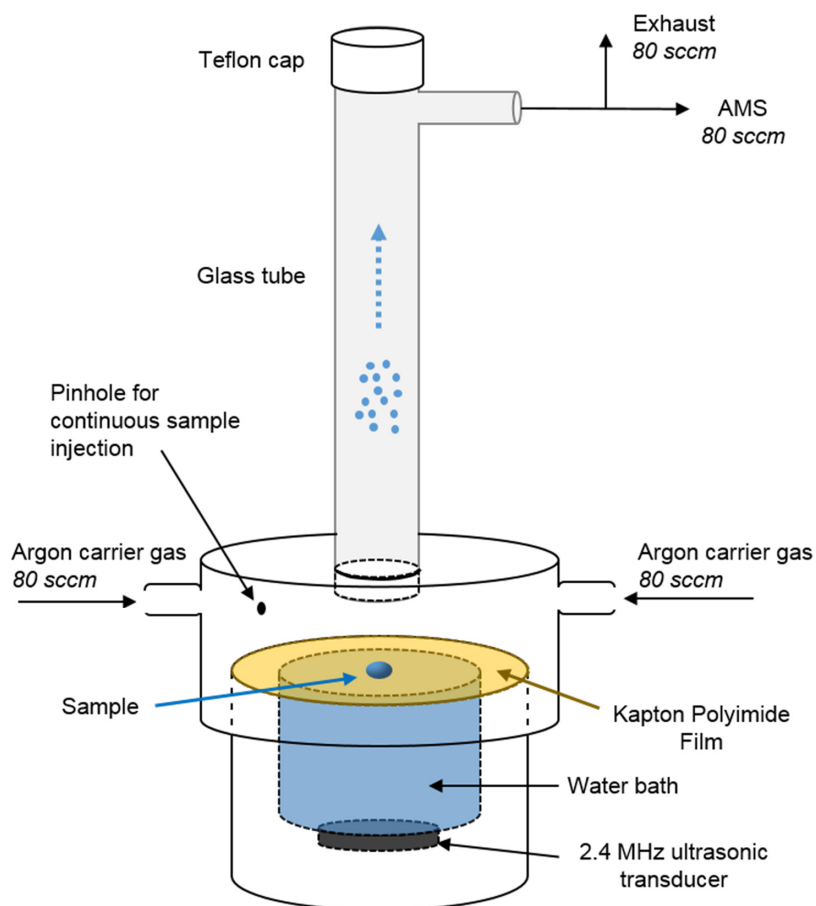
578 Table 1. Elemental ratios measured by SVN-AMS vs. other techniques for the various mixtures examined in this work.

Sample		O:C	H:C	N:C
Citric acid	Atomizer-AMS	1.0	1.4	--
	SVN-AMS	1.1	1.3	--
α -pinene SOA	Online-AMS	0.48	1.6	< 0.002
	SVN-AMS	0.50	1.6	< 0.002
Look Rock	Online-ACSM ^a	0.13 ($f_{44}=0.19$)	1.3 ($f_{43}=0.062$)	-- ^b
	SVN-AMS ^a	0.13 ($f_{44}=0.16$)	1.3 ($f_{43}=0.051$)	-- ^b
DOM	CHNS analyzer	ND	1.74	0.080
	SVN-AMS	0.77	1.7	0.081

579

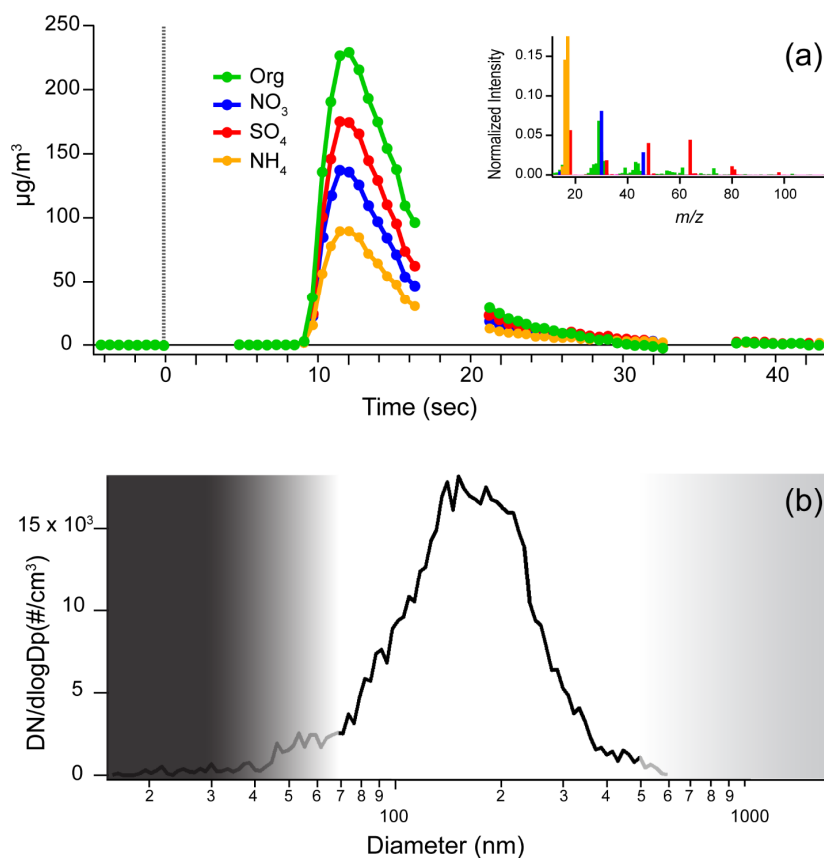
580 a. Elemental ratios are estimated from parameterizations for f_{44} and f_{43} (Aiken et al., 2008; Ng et al., 2011b).

581 b. There is no parameterization for N/C from UMR data.

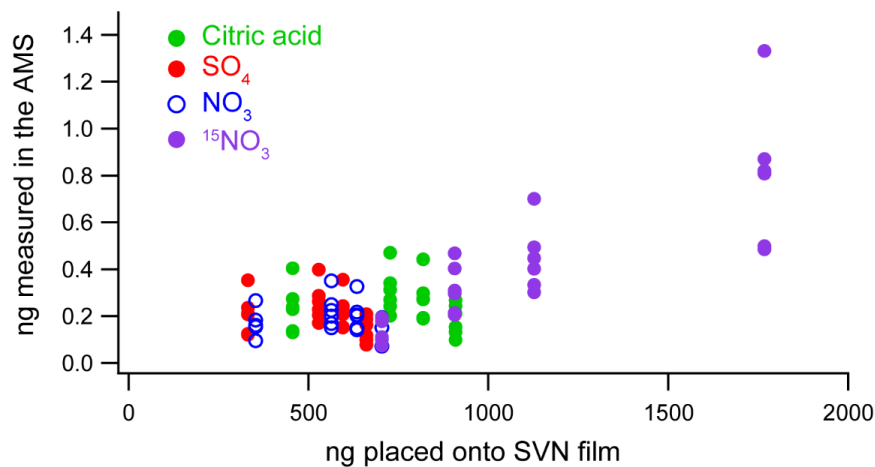


582

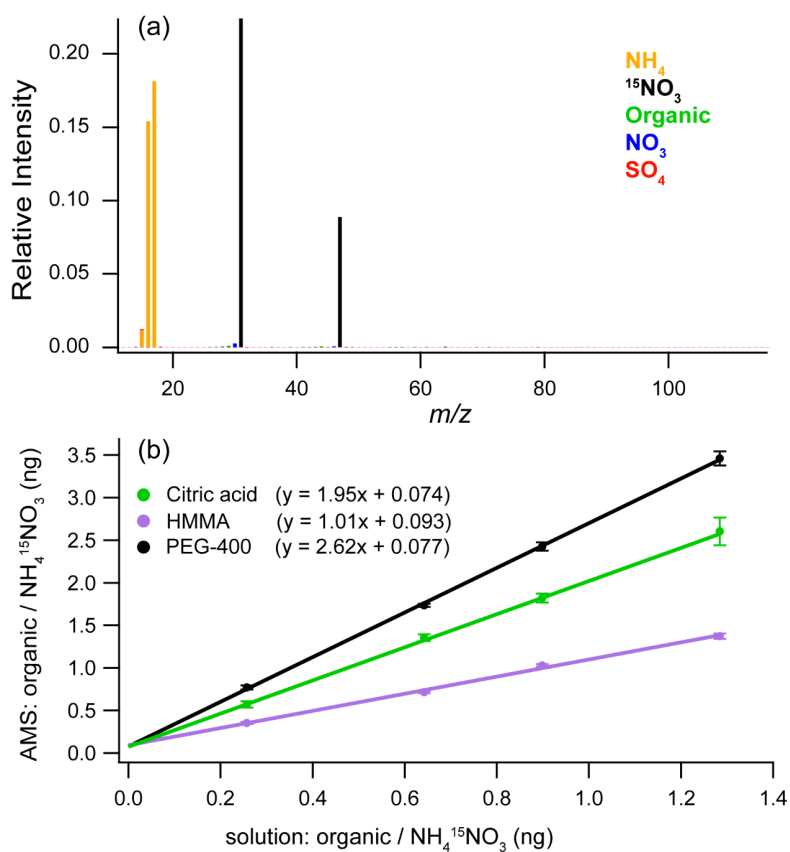
583 Figure 1. Schematic diagram of small volume ultrasonic nebulizer (SVN). Samples (2-4 μ L) are loaded on the Kapton (or
 584 Teflon) film through either the hole in which the glass tube is seated (for discrete injections) or through the pinhole (for
 585 continuous injections). After the transducer is turned on, the aerosol is carried up through the glass tube and into the
 586 instrument by a ~160 sccm flow of house air or argon carrier gas. The water bath between the transducer and the Kapton
 587 film carries ultrasonic waves up to the film and serves to cool the ultrasonic transducer.



588 Figure 2. Measurements of the composition and size of nebulized samples from the SVN. (a) Time series of aerosol
589 composition from a single 4 μL nebulization of an aqueous solution (mannitol, ammonium nitrate, and ammonium sulfate).
590 Data were recorded using fast-mode MS for the AMS-open scans, with a mass spectrum collected every 0.5 s (filled circles).
591 The gaps in the trace correspond to closed cycles where the aerosol beam was blocked to provide a background subtraction
592 (gas-phase and instrument background) that was applied during data processing. Measured concentrations are not
593 corrected for collection efficiency (CE) in the AMS, which affects the absolute values but not the relative concentrations.
594 The inset shows the average mass spectrum acquired across the injection, normalized to total ion signal. (b) Aerosol size
595 distribution from a $\sim 1\text{g/L}$ citric acid solution measured with an SMPS (black line). The gradient represents the
596 transmission efficiency for particles into the AMS with nearly 100% between 70-500 nm and decreased but substantial
597 transmission for spherical particles 30-70 nm and 500 nm to 2.5 μm (Jimenez et al., 2003); thus, the smallest particles in the
598 distribution will not be efficiently detected by the AMS.



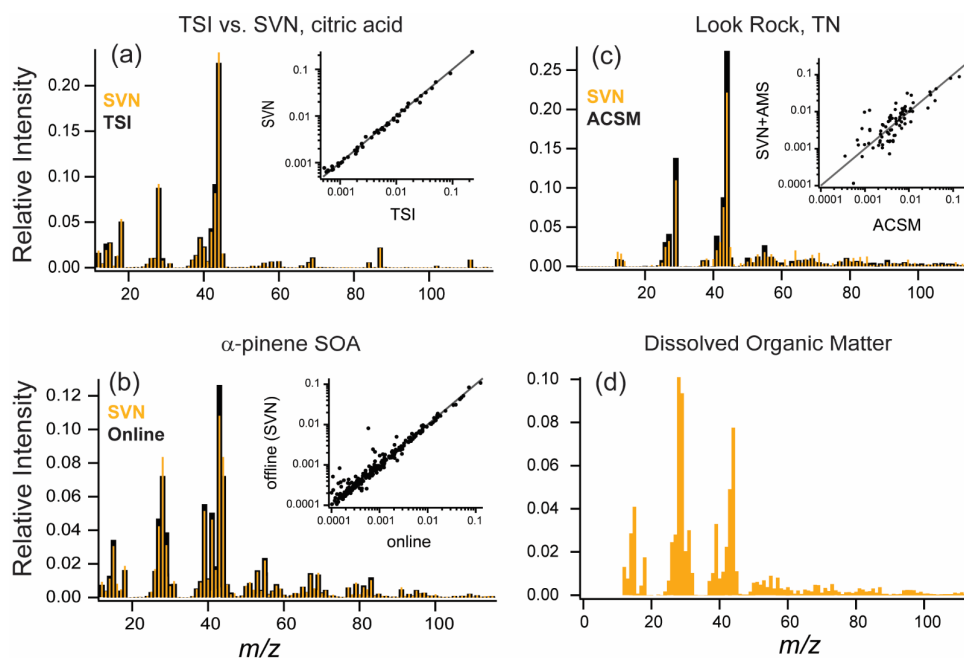
599 Figure 3. Mass of each component placed on the thin film vs. the mass measured by the AMS for 4 different solutions with
600 varying concentrations of citric acid, ammonium sulfate, ammonium nitrate, and the internal standard ($\text{NH}_4^{15}\text{NO}_3$), all
601 with a total solution concentration of 0.75 g/L. Each sample had 5 replicate injections, with the vertical spread in the
602 measured masses indicating substantial run-to-run variability (up to a factor of 3) between injections.



603 Figure 4. (a) Blank of the Kapton film using 1 g/L internal standard solution (^{15}N - ammonium nitrate). (b) Calibration
604 curves made using an internal standard for solutions with three different organic compounds: citric acid, 4-hydroxy-3-
605 methoxy-DL-mandelic acid (HMMA), and polyethylene glycol 400 (PEG-400). The error bars are $\pm 1\sigma$ for five replicate
606 injections.



607



608 **Figure 5.** Online (or TSI atomizer) (black) vs. SVN nebulizer (orange) mass spectra for (a) an aqueous solution of citric
609 acid at 1 g/L; (b) α -pinene + O₃ chamber SOA; (c) a SOAS campaign sample from Look Rock, TN with online data collected
610 on an ACSM. Smaller insets in a, b, and c show direct comparison of intensities for each mass spectrum on a log scale. (d)
611 AMS mass spectra from North Pacific Ocean dissolved organic matter nebulized with the SVN (since this sample was not
612 from aerosol particles, no online samples are available).